Implementation of a novel two-attractor grid multi-scroll chaotic system*

Luo Xiao-Hua(罗小华)[a)†], Tu Zheng-Wei(涂正伟)[a)], Liu Xi-Rui(刘希瑞)[a)], Cai Chang(蔡 昌)[a)], Liang Yi-Long(梁亦龙)[b)], and Gong Pu(龚 璞)[a)]

[a)] *College of Communication and Information Engineering, Chongqing University of Posts and Telecommunications, Chongqing* 400065, *China*

[b)] *College of Biological Information, Chongqing University of Posts and Telecommunications, Chongqing* 400065, *China*

(Received 3 November 2009; revised manuscript received 3 February 2010)

This paper proposed a method of generating two attractors in a novel grid multi-scroll chaotic system. Based on a newly generated three-dimensional system, a two-attractor grid multi-scroll attractor system can be generated by adding two triangular waves and a sign function. Some basic dynamical properties, such as equilibrium points, bifurcations, and phase diagrams, were studied. Furthermore, the system was experimentally confirmed by an electronic circuit. The circuit simulation results and numerical simulation results verified the feasibility of this method.

Keywords: chaos, grid multi-scroll attractor, two-attractor grid multi-scroll chaotic system, circuit simulation

PACC: 0545

1. Introduction

Since Lorenz found the first chaos model in 1963,[1] chaos has been deeply studied in many fields, including secret communication and information hiding, on which much attention has been focused. In 1984, Chua's circuit was found and has been widely studied as a paradigm of chaos and a bridge between electronic circuits and chaos theory.[2]

In 1993, Suykens first proposed a method for generating multi-scroll chaotic attractor.[3,4] Studies for generating multi-scroll chaotic attractor in Chua' circuit have become mature,[3−19] which drives the chaos system to generate a relevant number of scrolls through changing the number of turning points in the nonlinear functions. The existing nonlinear functions are piecewise linear function, step wave, sine function, time-lag function and so on.[5−10] They generated single scroll in one direction.

Single scroll of multi-scroll chaotic attractor in multiple directions can be generated by two or more nonlinear functions, such as the multi-folded torus system, grid multi-scroll Chua system, multi-directional multi-scroll chaotic system, ring-shaped multi-scroll generalised Lorenz system, and so on.[11−15]

At present, the grid multi-scroll[17−19] attractor is made up of several single scroll attractors. The defect is that it cannot generate two-attractor grid multi-scroll attractor. Is it possible to generate two-attractor grid multi-scroll attractor?

This paper proposes a two-attractor grid multi-scroll chaotic system. Based on a three-dimensional system, a novel two-attractor grid multi-scroll chaotic system is constructed by adding two triangular waves and a sign function. This system can generate two-attractor grid multi-scroll attractor in x and y directions. In this paper we briefly study and analyse its dynamical properties and behaviours, including calculation of equilibrium points and numerical simulation for bifurcation. Different kinds of phase diagrams of two-attractor grid multi-scroll attractor are obtained by controlling two kinds of nonlinear functions; the system exhibits the abundant and complex chaotic dynamic properties of two-attractor grid multi-scroll attractor. In the end, a chaotic circuit is designed. Through circuit simulation experiments, the results are found to be in agreement with those of numerical simulation.

*Project supported by the National Natural Science Foundation of China (Grant No. 60972069) and the Science and Technology Foundation of the Education Department of Chongqing (Grant No. KJ090513).

†Corresponding author. E-mail: luoxh_0630@yahoo.cn

© 2010 Chinese Physical Society and IOP Publishing Ltd

2. A novel three-dimensional system generating two-attractor grid multi-scroll chaotic attractor

This novel three-dimensional chaotic system was described as

$$\begin{cases} \dot{x} = az - bf_1(y), \\ \dot{y} = cz - h\mathrm{sgn}(z), \\ \dot{z} = df_2(x) - ez, \end{cases} \tag{1}$$

where $a = b = d = e = 1$, $c = 2$, $h = 0.8$, and x, y, z are state variables of the system. Nonlinear functions f_1, $f_2 \in \{f_{11}, f_{12}\}$ and

$$f_{11}(u) = \frac{1}{2\alpha} \sum_{\substack{m=-M \\ m\neq 0}}^{M} \left[\left| u - \left(2m - \frac{|m|}{m} \right) + \alpha \right| - \left| u - (2m - \frac{|m|}{m}) - \alpha \right| \right] - u, \tag{2}$$

$$f_{12}(u) = \frac{1}{2\alpha} \sum_{\substack{n=-N \\ n\neq 0}}^{N+1} \left[\left| u - \left(2n - \frac{|n|}{n} \right) + \alpha \right| - \left| u - (2n - \frac{|n|}{n}) - \alpha \right| \right] - u + 1, \tag{3}$$

where $\alpha = 0.02$ and $m, n \geq 0$.

According to formulas (1)–(3), the system can generate four kinds of two-attractor grid multi-scroll attractor as follows.

Let both $f_1(y)$ and $f_2(x)$ be $f_{11}(u)$. The chaotic system can generate $(2M+1) \times (2M+1)(M \geq 0)$ couple of grid multi-scroll attractors. The 3×3 grid multi-scroll attractor is described as an example in Fig. 1(a).

Let f_1(y) and $f_2(x)$ be $f_{12}(u)$ and $f_{11}(u)$ respectively. The chaotic system can generate $(2N+2) \times (2M+1)(M, N \geq 0)$ couple of grid multi-scroll attractors, and the 2×3 grid multi-scroll attractor is depicted as an example in Fig. 1(b).

Let both $f_1(y)$ and $f_2(x)$ be $f_{12}(u)$, the chaotic system can generate $(2N+2) \times (2N+2)(N \geq 0)$ couple of grid multi-scroll attractors. The 2×2 grid multi-scroll attractor is depicted as an example in Fig. 1(c).

Let $f_1(y)$ and $f_2(x)$ be $f_{11}(x)$ and $f_{12}(x)$ respectively. The chaotic system can generate $(2M+1) \times (2N+2)(M, N \geq 0)$ couple of grid double-scroll attractors, and the 3×2 grid multi-scroll attractor is depicted as an example in Fig. 1(d).

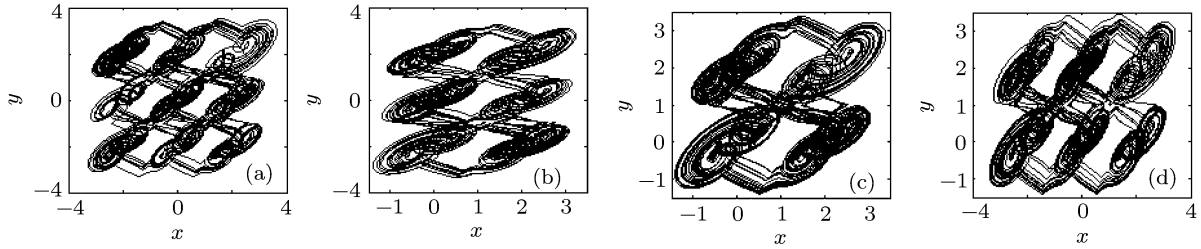


Fig. 1. Two-attractor grid multi-scroll attractors of Eq. (1) in $x - y$ plane (a) 3×3; (b) 2×3; (c) 2×2; (d) 3×2.

3. Basic dynamical behaviours

In order to obtain the system equilibrium points, let the right-hand side of Eq. (1) equal to zero. We can obtain

$$\begin{cases} z - f_1(y) = 0, \\ 2h(z) = 0, \\ f_2(x) - z = 0. \end{cases} \tag{4}$$

Based on Eq. (4), let both $f_1(y)$ and $f_2(x)$ be $f_{11}(u)$, the equilibrium points can be calculated by $(E_{-x,m} - 0.4,\ E_{-y,m} - 0.4,\ -0.4)$, $(E_{-x,m} + 0.4,\ E_{-y,m} + 0.4,\ 0.4)$, where $E_{-x,m} = 2m$, $(m = 0, \pm 1, \pm 2, \ldots, \pm M)$, $E_{-y,m} = 2m$, $(m = 0, \pm 1, \pm 2, \ldots, \pm M)$, generating $2\times(2M+1) \times (2M+1)$-scroll attractors. Let $M = 1$, then the 3×3 couple of two-attractor grid multi-scroll attractor can be obtained as shown in Fig. 2(a), where '•' denotes the equilibrium point of index 2. Thus, the number of the equilibrium points of index 2 is 2×3×3. Each equilibrium point can generate one scroll, so the number of scroll is 2×3×3.

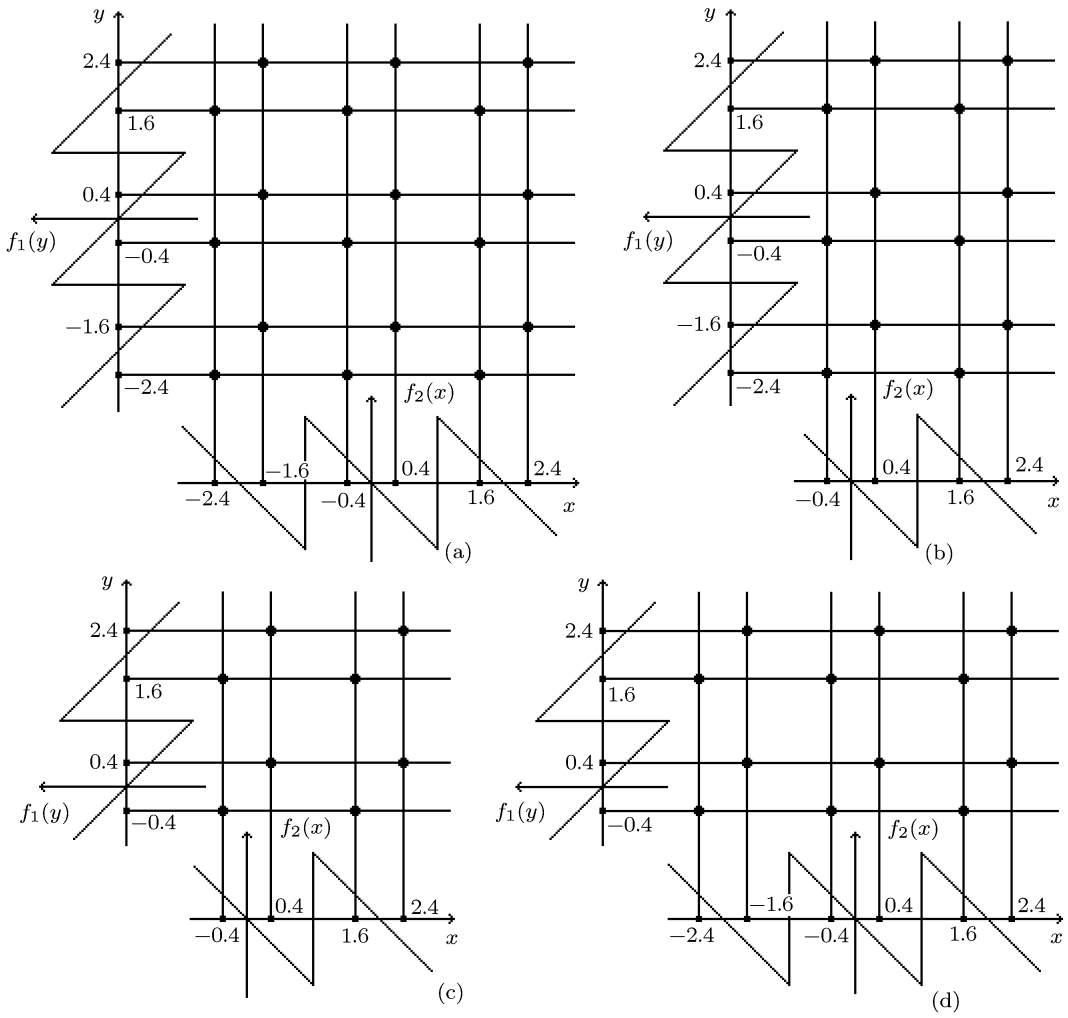


Fig. 2. The distribution of equilibrium points of Eq. (1) in $x-y$ plane, (a) 3×3 equilibrium points ; (b) 2×3 equilibrium points; (c) 2×2 equilibrium points; (d) 3×2 equilibrium points.

Based on Eq. (4), let $f_1(y)$ and $f_2(x)$ be $f_{12}(u)$ and $f_{11}(u)$ respectively. The equilibrium points can be calculated by $(E_{-x,m}-0.4,\ E_{-y,n}-0.4,\ -0.4)$, $(E_{-x,m}+0.4,\ E_{-y,n}+0.4,\ 0.4)$, where $E_{-x,m}=2m$, $(m=0,\pm1,\pm2,\ldots,\pm M)$, $E_{-y,n}=2n$, $(n=0,\pm1,\pm2,\ldots,\pm N,\pm(N+1)$, generating $2\times(2N+2)\times(2M+1)$-scroll attractors. Let $M=1$, $N=0$; the 2×3 couple of two-attractor grid multi-scroll attractor can be obtained, as shown in Fig. 2(b), where "•" denotes the equilibrium point of index 2. Thus, the number of the equilibrium points of index 2 is 2×2×3. Each equilibrium point can generate one scroll, so the number of scroll is 2×2×3.

Based on Eq. (4), let both $f_1(y)$ and $f_2(x)$ be $f_{12}(u)$, the equilibrium points can be calculated by $(E_{-x,n}-0.4,\ E_{-y,n}-0.4,\ -0.4)$, $(E_{-x,n}+0.4,\ E_{-y,n}+0.4,\ 0.4)$, where $E_{-x,n}=2n$, $(n=0,\pm1,\pm2,\ldots,\pm N,\pm(N+1))$, $E_{-y,n}=2n$, $(n=0,\pm1,\pm2,\ldots,\pm N,\pm(N+1))$, generating $2\times(2N+2)\times(2N+2)$-scroll attractors. Let $N=0$, 2×2 couple of two-attractor grid multi-scroll attractors can be obtained as shown in Fig. 2(a), where '•' denotes the equilibrium point of index 2. Thus, the number of the equilibrium points of index 2 is 2×2×2. Each equilibrium point can generate one scroll, so the number of the scroll is 2×2×2.

Based on Eq. (4), let $f_1(y)$ and $f_2(x)$ be $f_{11}(x)$ and $f_{12}(x)$ respectively, the equilibrium points can be calculated as $(E_{-x,n}-0.4,\ E_{-y,m}-0.4,\ -0.4)$, $(E_{-x,n}+0.4,\ E_{-y,m}+0.4,\ 0.4)$, where $E_{-x,n}=2n$, $(n=0,\pm1,\pm2,\ldots,\pm N,\pm(N+1))$, $E_{-y,m}=2m$, $(m=0,\pm1,\pm2,\ldots,\pm M)$, generating $2\times(2M+1)\times(2N+1)$-scroll attractors. Let $M=1$, $N=0$, 3×2 couple of two-attractor grid multi-scroll attractor can

be obtained as in Fig. 2(a), where '•' stands for the equilibrium point of index 2. Obviously, the number of the equilibrium points of index 2 was 2×3×2. Each equilibrium point can generate one scroll, so the number of the scroll was 2×3×2.

According to formulas (1)–(3), the Jacobi matrix of the equilibrium point of index 2 can be obtained

$$\boldsymbol{J} = \begin{pmatrix} 0 & -k & 1 \\ 0 & 0 & u \\ k & 0 & -1 \end{pmatrix}.$$

The corresponding characteristic equation is $\lambda^3 + \lambda^2 - k\lambda + uk^2 = 0$. Let $k = -1$, $u = 2$. The latent roots can be obtained as $\lambda_{1,2} = 0.1766 \pm 1.2028\mathrm{i}$, $\lambda_3 = -1.3532$, confirming that the equilibrium points expressed as "•" in Figs. 2(a)–2(d) are the equilibrium points of index 2.

Let both $f_1(y)$ and $f_2(x)$ be $f_{11}(u)$ and choose $M = 1$. The bifurcation diagram of state variable x, which varies with α, is shown in Fig. (3). Thus, the system presents a chaotic state for $\alpha \in (0, 0.35)$.

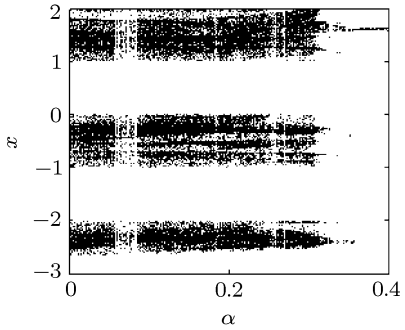


Fig. 3. The bifurcation x versus α.

4. Design of two-attractor grid multi-scroll chaotic circuit and its simulation

In the circuit design, we used linear resistors, capacitors and operating amplifiers. All the operating amplifiers were of type TL082CD and their saturation value was $|V_{\mathrm{sat}}| = 13.5$ V.

The circuit of triangular waves was designed according to formulas (2) and (3); the circuits of sign function and the two-attractor grid multi-scroll chaotic system were designed according to Eq. (1). In the end, the circuit simulation results of 3×3, 2×3, 2×2 and 3×2 couples of two-attractor grid multi-scroll attractors were presented.

4.1. Circuit design of triangular waves $f_{11}(u)$ and $f_{12}(u)$

According to formulas (2) and (3), let $M = 1$, $N = 0$. The triangular waves $f_{11}(u)$ and $f_{12}(u)$ were designed as shown in Fig. 4.

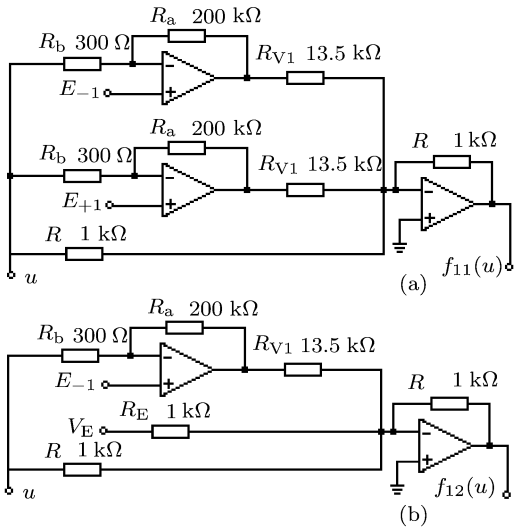


Fig. 4. Circuit design of triangular waves, (a) $f_{11}(u)$, (b) $f_{12}(u)$.

In Fig. 4, $R_{\mathrm{VI}} = 13.5$ kΩ is the resistance for voltage–current conversion, R_{E} is a balance resistance under the additional voltage V_{E}, with $R_{\mathrm{E}} = 1$ kΩ, $V_{\mathrm{E}} = 1$ V. The parameter α is determined by R_{a}, R_{b}, and their conjoint amplifier, $\alpha = R_{\mathrm{b}} \times |V_{\mathrm{sat}}|/R_{\mathrm{a}}$. For $|V_{\mathrm{sat}}| = 13.5$ V and $\alpha = 0.02$, we choose $R_{\mathrm{a}} = 200$ kΩ, $R_{\mathrm{b}} = 300$ Ω. R_{a}, R_{b}, and linear resistance R are used for producing positive slope line of the triangular wave, while linear resistance R is used also for producing negative slope line of the triangular wave. $E_{\pm 1} = \pm 1$ V is the voltage of the equilibrium points in the positive slope line of the triangular wave.

Figure 4(a) shows the circuit of triangular wave $f_{11}(u)$. Let the input be u or $-u$, and the output be $f_{11}(u)$ or $-f_{11}(u)$. Figure 4(b) shows the circuit of triangular wave $f_{12}(u)$, with the input being u or $-u$, and the output $f_{12}(u)$ or $-f_{12}(u)$.

4.2. Circuit design of sign function

By utilizing the inherent nonlinear specialty of amplifier, we have designed the sign function shown in Fig. 5. In Fig. 5, as the voltage of reversed input changes smoothly from negative to positive, the voltage of output will jump from the positive saturation to the negative one; when it is changed from positive

to negative, the output will jump from negative to positive.

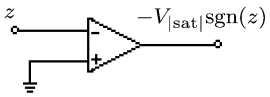


Fig. 5. Design of sign function.

4.3. Circuit design of the two-attractor grid multi-scroll chaotic system

By utilizing Eq. (1), the circuit was designed as shown in Fig. 6.

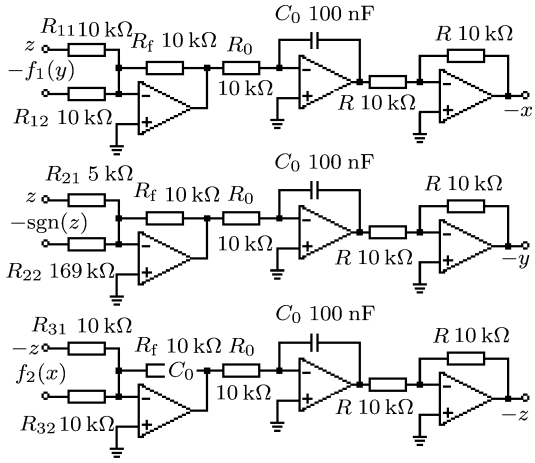


Fig. 6. Two-attractor grid multi-scroll chaotic circuit.

According to Eq. (1) and circuit in Fig. 6, the circuit equation can be obtained as follows:

$$\begin{cases} \dfrac{\mathrm{d}x}{\mathrm{d}\tau} = -R_{\mathrm{f}}\left[\dfrac{z}{R_{11}} - \dfrac{f_1(y)}{R_{12}}\right], \\ \dfrac{\mathrm{d}y}{\mathrm{d}\tau} = -\dfrac{R_{\mathrm{f}}}{R_{21}}z + \dfrac{|V_{\mathrm{sat}}|R_{\mathrm{f}}}{R_{22}}\mathrm{sgn}(z), \\ \dfrac{\mathrm{d}z}{\mathrm{d}\tau} = -R_{\mathrm{f}}\left[\dfrac{f_2(x)}{R_{32}} - \dfrac{z}{R_{31}}\right]. \end{cases} \tag{5}$$

From Eq. (1), we have $a = R_{\mathrm{f}}/R_{11}$, $b = R_{\mathrm{f}}/R_{12}$, $c = R_{\mathrm{f}}/R_{21}$, $e = R_{\mathrm{f}}/R_{31}$, $d = R_{\mathrm{f}}/R_{32}$, $h = R_{\mathrm{f}} \times |V_{\mathrm{sat}}|/R_{22}$. Let $R = R_{\mathrm{f}} = 10$ kΩ, and $a = b = d = e = 1$, $c = 2$, $h = 0.8$. We have $R_{11} = R_{12} = R_{31} = R_{32} = 10$ kΩ, $R_{21} = 5$ kΩ, $R_{22} = 169$ kΩ. The time constant $\tau = t/(R_0C_0)$, where $1/(R_0C_0)$ is the integral constant of the integrator. In the experiment, we have choosen $R_0 = 10$ kΩ, $C_0 = 100$ nF.

4.4. Results of circuit simulation

Let the output signal $-\mathrm{sgn}(z)$ in Fig. 5 be connected to the input signal $-\mathrm{sgn}(z)$ in Fig. 6.

Let the input signal in Fig. 4(a) be $-y$, so that the output is $-f_{11}(y)$, connected to the input signal $-f_1(y)$ in Fig. 6. Meanwhile, let the input signal in Fig. 4(a) be x, so that the output is $f_{11}(x)$, connected to the input signal $f_2(x)$ in Fig. 6. And then the circuit simulation diagram of 3×3 couple of two-attractor grid multi-scroll attractor can be obtained as shown in Fig. 7(a).

Let the input signal in Fig. 4(a) be $-y$, so that the output is $-f_{11}(y)$, connected to the input signal $-f_1(y)$ in Fig. 6. Meanwhile, let the input signal in Fig. 4(b) be x, so that the output is $f_{12}(x)$, connected to the input signal $f_2(x)$ in Fig. 6. And then the circuit simulation diagram of 2×3 couple of two-attractor grid multi-scroll attractor can be obtained as shown in Fig. 7(b).

Let the input signal in Fig. 4(b) be $-y$, so that the output is $-f_{12}(y)$, connected to the input signal $-f_1(y)$ in Fig. 6. Meanwhile, let the input signal in Fig. 4(b) be x, so that the output is $f_{12}(x)$, connected to the input signal $f_2(x)$ in Fig. 6. And then the circuit simulation diagram of 2×2 couple of two-attractor grid multi-scroll attractor can be obtained as shown in Fig. 7(c).

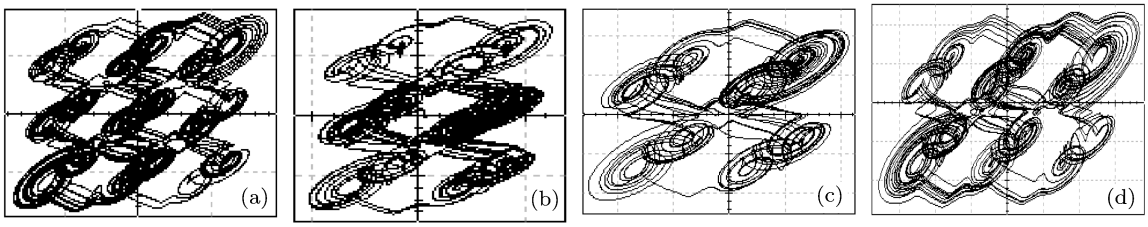


Fig. 7. Circuit simulation results of two-attractor grid multi-scroll attractor of Eq. (1) in x–y plane. The multi-scroll attractors are: (a) 3×3; (b) 2×3; (c) 2×2; (d) 3×2.

Let the input signal in Fig. 4(b) be $-y$, so that the output is $-f_{12}(y)$, connected to the input signal $-f_1(y)$ in Fig. 6. Meanwhile, let the input signal in Fig. 4(a) be x, so that the output is $f_{11}(x)$, connected to the input signal $f_2(x)$ in Fig. 6. And then the circuit simulation diagram of 3×2 couple of two-attractor grid multi-scroll attractor can be obtained as shown in Fig. 7(d).

From above information, the circuit simulation results are in agreement with numerical simulations.

5. Conclusions

In this paper, a novel three-dimensional two-attractor grid multi-scroll chaotic system has been proposed. Some basic dynamical behaviours, such as equilibrium points, bifurcations and phase diagram have been further investigated, confirming that it is capable to generate a two-attractor grid multi-scroll attractor by constructing two triangular waves and a sign function. In the end, the success of the design has been verified by circuit simulation results, which are in agreement with numerical simulations. The system exhibits complex chaotic dynamics, showing that if may have potential applications in engineering.

References

[1] Lorenz E N 1963 *J. Atmos. Sci.* **20** 130

[2] Matsumoto T, Chua L O and Komuro M 1985 *IEEE Trans. CAS* **32** 798

[3] Suykens J and Vandewalle J 1993 *IEEE Trans. CAS2* I **40** 861

[4] Yalcin M E, Suykens J and Vandewalle J 2000 *IEEE Trans. CAS2* I **47** 425

[5] Tang W K S, Zhong G Q, Chen G and Man K F 2001 *IEEE Trans. CAS* I **48** 1369

[6] Zhong G Q, Man K F and Chen G R *Int. J. Bifurc. Chaos* **12** 2907

[7] Yu S M, Qiu S S and Lin Q H 2003 *Sci. Chin.* F **46** 104

[8] Elwakil A S and Kennedy M P 2000 *Int. J. Circ. Theor. Appl.* **28** 319

[9] Yu S M, Lin Q H and Qiu S S 2004 *Acta Phys. Sin.* **53** 2084 (in Chinese)

[10] Yu S M, Ma Z G, Qiu S S, Peng S G and Lin Q H 2004 *Chin. Phys.* **13** 317

[11] Lü J H, Han F, Yu X and Leung H 2004 *IEEE Trans. Circuits Syst.* I **51** 2476

[12] Yu S M, Lü J H and Chen G R 2007 *IEEE Trans. Circuits Syst.* I **54** 2087

[13] Yu S M, Lü J H and Chen G R 2007 *Chaos* **17** 013118

[14] Yu S M, Tang K S and Chen G R 2007 *Int. J. Bifur. Chaos* **17** 3951

[15] Liu F, Liu S D, Liu G and Liu S K 2007 *Acta Phys. Sin.* **56** 5629 (in Chinese)

[16] Wang F Q, Liu C X and Lu J J 2006 *Acta Phys. Sin.* **55** 3289 (in Chinese)

[17] Yu S M 2005 *Acta Phys. Sin.* **54** 1500 (in Chinese)

[18] Zhang Z X and Yu S M 2009 *Acta Phys. Sin.* **58** 120 (in Chinese)

[19] Wang F Q and Liu C X 2007 *Acta Phys. Sin.* **56** 1983 (in Chinese)